10.2478/v10170-011-0042-y

Archives of Control Sciences
Volume 23(LIX), 2013
No. 1, *pages 61–78*

Robust control system design in frequency domain

VOJTECH VESELÝ and JAKUB OSUSKÝ

In this paper two robust control methods for hybrid system are presented. Both methods are usefull for SISO and MIMO systems. Controller design procedure is developed in frequency domain. Equivalent subsystem method is used for controller design in this paper. Stability condition of proposed methods bases on small gain theory and uses additive and inverse additive model type. Two tank water system is presented in the paper and serves as a numerical example to compare effectiveness of described methods.

Key words: hybrid control, equivalent subsystem method, PI controller

1. Introduction

The topic of hybrid control has attracted considerable attention from the industrial and research community in recent decade. Wherever continues and discrete dynamics interacts, hybrid system arises and theory of hybrid system is used. This theory studies behavior of dynamical systems which involves continuous-time models represented by differential or difference equations describing physical, mechanical or chemical plants and discrete models such as finite state machines or Petri nets which show the software and logical behavior.

There are several approaches to model hybrid systems [6]. In [1] model of a large class of hybrid systems is considered as a discrete event system. Continuous dynamics is modeled by differential or difference equation. Such models are used to formulate a general stability analysis and controller synthesis framework for hybrid systems. Results for modeling and stability analysis of hybrid systems have been presented in [7], [3] and [6]. In the present paper, we follow the class of hybrid system known as switched systems [5]. The survey of the actual state of hybrid systems can be found in excellent works [7] and [6].

In the present paper, stability and controller design problems are solved using Lyapunov stability theory [2], [8]. Robust controller design using small gain theory and its unification for SISO and MIMO systems is proposed. Two robust controller design meth-

The Authors are with the Institute of Control and Industrial Informatics, Slovak University of Technology in Bratislava, Ilkovicova 3, 812 19 Bratislava. E-mail: {vojtech.vesely,jakub.osusky}@ stuba.sk

The work on this paper is supported by VEGA 1/1105/11 and APVV-0211-10.
Received 31.08.2012. Revised 14.12.2012.

ods are presented and compared. In the first method, robust controller which guarantees robust properties of hybrid system is designed. Using second method, robust controller is designed for each mode of hybrid system. In the first case nominal model is calculated as average one according to all modes and in second case for each mode nominal model and uncertainty model is calculated. According to greater number of nominal models, second method can be more conservative.

2. Problem formulation

Consider MIMO hybrid uncertain system described by a set of transfer function matrices $G_q(s) \in \Re^{m\times m}$ and controller $R_q(s) \in \Re^{m\times m}$ in the standard configuration (shown in Fig. 1), where $y(s) \in \Re^l$, $u(s) \in \Re^m$ and $w(s) \in \Re^l$ are output, control and setpoint

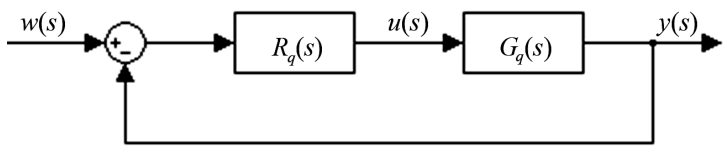

Figure 1. Standard feedback control configuration.

variables of system, respectively. Parameter $q = 1,2,...,N$ represents number of switched modes of uncertain system and q indicates the arbitrary switching algorithm for switched system.

Assume that throughout the practical identification undertaken for each mode q one obtains K transfer function matrices. To deal with uncertainties in mode q with the nominal transfer function matrix, uncertainty model is used. Instead of a single model, the class of models is considered. For each mode q, the $G_{qj}(s) \in \Pi_q$, $j = 1,2,...,K$ represents member of a set of possible plants. All K transfer function matrices creates a set $\Pi_q \in \Pi$, thus any transfer function matrix belongs to the set Π:

$$G_{qj}(s) \in \Pi, \;\; q = 1,2,...,N, \;\; j = 1,2,...,K. \tag{1}$$

A simple uncertainty model is obtained using unstructured model approach. In the sequel, two most common single uncertainty models are considered: additive and inverse additive model type [9]. Corresponding classes of uncertain models are given as follows.

1) Additive uncertainty model for mode $q = 1,2,...,N$

$$G_{qu}(s) = G_q(s) + \Delta_a(s)W_a(s) \tag{2}$$

where

$$l_a(\omega) = \max_{G_{ij} \in \Pi_i} \sigma_M[G_{ij}(s) - G_i(s)] \;\; i = 1,2,...,N, \;\; j = 1,2,...,K \tag{3}$$

and $|W_a(s)| \geqslant l_a(s)$.

2) Inverse additive uncertainty model for mode $q = 1,2,...,N$

$$G_{qu}(s) = (G_q(s)\Delta_{ia}(s)W_{ia}(s) + I)^{-1} G_q(s) \tag{4}$$

where

$$l_{ia}(\omega) = \max_{G_{ij} \in \Pi_i} \sigma_M[G_{ij}(s)^{-1} - G_i(s)^{-1}] \;\; i = 1,2,...,N, \;\; j = 1,2,...,K \tag{5}$$

and

$$|W_{ia}(s)| \geqslant l_{ia}(s), \sigma_M(\Delta_a(s)) \leqslant 1, \sigma_M(\Delta_{ia}(s)) \leqslant 1 \;\; \forall s \in D \tag{6}$$

where D is Nyquist contour [9].

Consider MIMO switched uncertain system with N modes described by (1) for stable transfer function matrices, or by (2) for unstable ones. The problem is to design robust decentralized controller for switched system (1) or (2) and also control design unification for SISO and MIMO for two cases:

a) design of robust decentralized controller $R(s) \in \Re^{mxm}$ which guarantee the robust stability and performance for switched system in all modes, that is for $i = 1,2,...,N$.

b) For each mode design robust decentralized controllers $R_q(s)$, $q = 1,2,...,N$ such that guarantee the robust stability and performance for switched system in all modes $q = 1,2,...,N$ and over the entire operating range specified by uncertain models 1) or 2).

In derivation stability condition of systems with uncertainty, small gain theorem and generalized Nyquist stability theorem play important role. From Fig. 1 with uncertain model 1) or 2), after simple manipulation one can obtain $M - \Delta$ structure as shown in Fig. 2.

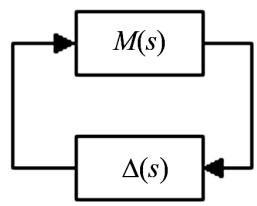

Figure 2. $M - \Delta$ structure.

Theorem 1 (small gain theorem) *Suppose $M(s)$ is stable and let $\gamma > 0$. Then the interconnected system shown in Fig. 2 is well-posed and internally stable for all $\Delta(s) \in \Re^{m\times m}$ if and only if*

$$||\Delta(s)||_\infty \leqslant ||_\gamma \quad \text{and} \quad ||M(s)||_\infty < \gamma \tag{7}$$

$$||\Delta(s)||_\infty < ||_\gamma \quad \text{and} \quad ||M(s)||_\infty \leqslant \gamma. \tag{8}$$

3. Theoretical results

3.1. Robust decentralized controller design for switched systems, case A

The problem is to design robust decentralized controller $R(s) = \text{diag}\{\Re_j(s)\}$, $j = 1,2,...,m$ which guarantees the closed loop stability for all modes and over the entire operating range specified by 1) or 2). For this special case we are given $N \times K$ plant transfer matrices with nominal model $G_u(s) \in \Re^{m\times m}$ and additive 1) or inverse additive 2) uncertainty model. The following generalized Nyquist theorem determines the closed-loop stability for nominal plant model.

Theorem 2 *The feedback system in Fig. 1 with nominal model $G(s)$ and controller $R(s)$ is stable if and only if $\forall s \in D$*

$$\det[I + G(s)R(s)] \neq 0 \tag{9}$$

$$N[0; \det[I + G(s)R(s)]] = n_f \tag{10}$$

where n_f is the number of unstable poles of $L(s) = G(s)R(s)$ and $N[0;\ \det[I + L(s)]]$ denotes the number of anticlockwise encirclement of origin $(0,0)$ by the Nyquist plot of $\det[I + L(s)]$.

For the case A the robust switched controller design procedure is based on the Equivalent Subsystem Method [4]. In the sequel introduce the following definition and theorem.

Definition 1 *For the nominal plant model $G(s)$ equivalent subsystem is given as*

$$G_{de}(s) = G_d(s) - P(s) = \text{diag}\{G_{ie}(s)\}_{m\times m} \tag{11}$$

where

$$G(s) = G_d(s) + G_m(s), G_d(s) = \text{diag}\{G(s)\}_{m\times m} \tag{12}$$

and $P(s) = p_i I$ is a characteristic function of the matrix $-G_m(s)$ that is

$$\det[p_i I + G_m(s)] = 0, \quad i = 1,2,...,m. \tag{13}$$

Using definition 1 and theorem 2 the following closed-loop stability conditions are obtained for nominal model.

Theorem 3 *Closed-loop system with nominal model and decentralized controller $R(s)$ is stable if and only if:*

$$\det[p_i I + G_m(s)] = 0, \quad i = 1,2,...,m, \tag{14}$$

characteristic polynomials of equivalent subsystem

$$I + R_i(s)G_{ie}(s) = 0 \tag{15}$$

is stable for all $i = 1,2,...,m$, and

$$N[0;\ \det[P(s) + G_m(s)] = n_f. \tag{16}$$

Equation (14) is the characteristic equation of the matrix $-G_m(s)$ with respect to p_i. Due to Cayley-Hamilton theorem, p_i in characteristic polynomial (14) can be replaced by $p_i I = -G_m(s)$ and stability condition in theorem 2 reduces to the stability of the following diagonal matrix

$$\det[R^{-1}(s) + G_d(s) - P(s)]. \tag{17}$$

Theorem 3 is the base to design the decentralized controller for the nominal model $G(s)$. Now let us consider the uncertain model with additive type uncertainty (2) for all system

$$G_u(s) = G(s) + \Delta_a(s)W_a(s) \tag{18}$$

where

$$l_a(\omega) = \max \sigma_M(G(s) - G_{ij}(s)). \tag{19}$$

By generalized Nyquist theorem the robust closed-loop stability is given as follows:

$$\begin{aligned} &\det[R(s)^{-1} + G_d(s) + G_m(s) + \Delta_a(s)W_a(s)]\det R(s) = \\ &\det[I + (G_d(s) - P(s))R(s) + \Delta_a(s)W_a(s)R(s)] = \\ &\det[I + G_{de}(s)R(s)]\det[I + (I + G_{de}(s)R(s))^{-1}\Delta_a(s)W_a(s)R(s)]. \end{aligned} \tag{20}$$

Suppose that condition (15) in theorem 2 holds, then robust closed loop system stability for additive type uncertainty is given as follows.

Theorem 4 *Closed-loop uncertain system with additive uncertainty type is stable if and only if:*

a) The nominal model with equivalent subsystems and decentralized controller $R(s)$ is stable, that is

b) $\det[I + G_{de}(s)R(s)] \neq 0$

c) and

$$N[0, \det[I + G(s)R(s)] = n_f. \tag{21}$$

d) The following robust stability conditions hold for $\forall s \in D$

$$||(I + G_{de}(s)R(s))^{-1}R(s)W_a(s)|| < 1 \tag{22}$$

or

$$||T_{oe}(s)|| < \left|\left|\frac{G_{de}(s)}{W_a(s)}\right|\right| \tag{23}$$

where

$$T_{oe}(s) = G_{de}(s)R(s)(I + G_{de}(s)R(s))^{-1}. \tag{24}$$

Because (23) is diagonal matrix, the condition (23) needs to be fulfilled for all equivalent subsystems with the controller $R(s)$. Note, that for for SISO systems $G_{de}(s) = G_d(s)$.

Closed-loop system with inverse additive uncertainty type is presented in Fig. 3 where

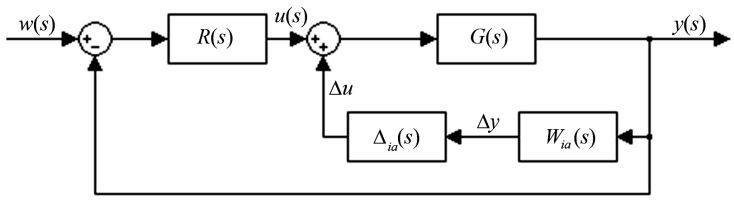

Figure 3. Closed-loop system with inverse additive uncertainty type.

$$l_{ia}(\omega) = \max_{G_{ij} \in \Pi} \sigma_M(G(s)^{-1} - G_{ij}(s)^{-1}). \tag{25}$$

After a simple manipulation one obtains from Fig. 3

$$\Delta y(s) = (I + G(s)R(s))^{-1}G(s)W_{ia}(s)\Delta u(s) = M_{ia}(s). \tag{26}$$

Figure 3 can be easily transformed to $M - \Delta$ structure with $M(s) = M_{ie}(s)$. Due to Theorem 1 the following corollary is hold.

Corollary 1 *The uncertain closed-loop system* (Fig. 3) *is stable if and only if*

$$||(I + G(s)R(s))^{-1}G(s)W_{ia}(s)|| < 1 \tag{27}$$

or after some manipulation

$$||S_e(s)|| < \left|\left|\frac{G_{de}(s)^{-1}}{W_{ia}(s)}\right|\right| \tag{28}$$

where

$$S_e(s) = (I + G_{de}(s)R(s))^{-1}. \tag{29}$$

Due to diagonal form of (15), the above conditions need to be fulfilled for all equivalent subsystems. The design procedure of the robust switched controller for the case A can be then summarized as follows.

1. For stable or unstable nominal model plant $G(s)$ calculate the characteristic functions $p_i(s)$, $i = 1,2,...,m$.

2. For the chosen $p_i(s)$ the equivalent subsystem transfer function is determined. Chosen $p_i(s)$ may guarantee the stability and maximal phase margin value for all equivalent subsystems.

3. For the nominal stable and unstable plant, functions $l_a(\omega)$ and respective $l_{ia}(\omega)$ are obtained.

4. From the functions $l_a(\omega)$ ($l_{ia}(\omega)$) the maximal value of complementary sensitivity function (sensitivity function) is determined

$$M_T = \max_{\omega}(T_{oe}(\omega)), \quad M_S = \max_{\omega}(S_{oe}(\omega)) \tag{30}$$

in such a way that

$$1 \leqslant M_T < l_a(\omega), \quad (M_S < l_{ia}(\omega)). \tag{31}$$

5. From known M_T (M_S) the minimal value of phase margin P_M is calculated [9]

$$P_M > 2\arcsin\left(\frac{1}{2M_T}\right), \quad P_M > 2\arcsin\left(\frac{1}{2M_S}\right). \tag{32}$$

6. Design the robust decentralized controller for all equivalent subsystems with performance determined by phase margin P_M.

7. For all closed-loop equivalent subsystems check the robust stability condition (23). If the robust stability condition is not satisfied, phase margin P_M is increased and robust controller calculation is performed again.

Note that for SISO systems points 1. and 2. of the algorithm are omitted.

3.2. Robust decentralized controller design for switched systems, case B

In the case B, for each mode of the switched system with arbitrary switch algorithm, robust decentralized controller $R_q(s)$, $q = 1,2,...,N$ is designed. Controller guarantees the robust stability and performance for all modes and over the entire operating range specified by uncertain models (2) or (4).

For the mode q, let the nominal model $G_p(s)$ and uncertainty model are calculated from transfer matrices $G_{qj}(s)$, $q = 1,2,...,N$, $j = 1,2,...,K$. The switching process can

change the mode q of the plant to any other mode $q+1$ from the set $\{1,...,N\}$. To guarantee the robust stability the equations (2) and (4) need to be modified as follows

$$G_{qu}^{q+1}(s) = G_q(s) + W_a^q(s)\Delta_q(s) \tag{33}$$

where

$$l_a^q(\omega) = \max_{G_{ij}(s)\in\Pi} \sigma_M(G_q(s) - G_{ij}(s)), \quad q = 1,2,...,N \tag{34}$$

$$|W_a^q(s)| \geqslant l_a^q(\omega) \tag{35}$$

and for inverse case

$$G_{qu}^{q+1}(s) = (G_q(s)\Delta_{ia}^q(s)W_{ia}^q(s) + I)^{-1}G_q(s) \tag{36}$$

where

$$l_{ia}^q(\omega) = \max_{G_{ij}(s)\in\Pi} \sigma_M(G_{ij}(s)^{-1} - G_q(s)^{-1}), \quad q = 1,2,...,N \tag{37}$$

Robust controller design procedure for switched system and each mode $q = 1,2,...,N$ goes the same way as for case A but instead of $l_a(\omega)$ and $l_{ia}(\omega)$ one needs to use (34) and (37).

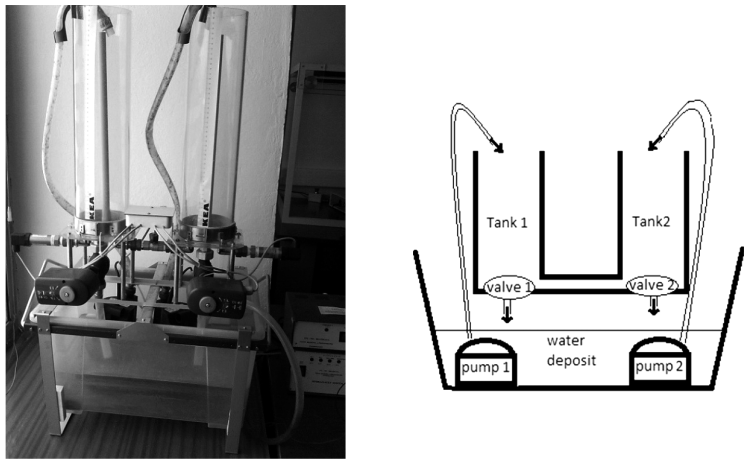

Figure 4. Two tanks process.

4. Example

Consider two tanks process with two inputs (pumps voltage) and two outputs (water level) depicted in Fig. 4. Process contains also valves which are used for decreasing water level in tanks. The voltage which controls the valves can be changed in the range

(0-10V). Different operating points were obtained by setting the voltage to 7.5V, 8.5V and 9.5V. A bottom pipe connects the tanks which allows water to flow from tank with higher level to tank with lower level and creates interaction between the tanks. Mode 1 represents the state with higher level in the tank 1. Similarly, mode 2 represents the state with higher level in the tank 2. The aim of the controller design is the robust control without overshoot. Transfer function matrices for both modes are given below. Note that upper index of the transfer function matrix denotes the mode number for which the identification was made. Lower index denotes the operating point which follows from the voltage applied to the valves: 7.5V (index 1), 8.5V (index 2) and 9.5V (index 3).

Model 1

$$
\begin{aligned}
G_1^1(s) &= \begin{bmatrix} \dfrac{0.049\mathrm{s}+0.98}{109.2\mathrm{s}^2+11.83\mathrm{s}+1} & \dfrac{-0.3}{25\mathrm{s}+1} \\ \dfrac{0.3}{25s+1} & \dfrac{0.059\mathrm{s}+1.19}{27.78\mathrm{s}^2+10.91\mathrm{s}+1} \end{bmatrix} \\
G_2^1(s) &= \begin{bmatrix} \dfrac{0.049\mathrm{s}+0.97}{46.5\mathrm{s}^2+8.76\mathrm{s}+1} & \dfrac{-0.4}{25\mathrm{s}+1} \\ \dfrac{0.4}{25s+1} & \dfrac{0.048\mathrm{s}+0.96}{61.06\mathrm{s}^2+11.41\mathrm{s}+1} \end{bmatrix} \\
G_3^1(s) &= \begin{bmatrix} \dfrac{0.047\mathrm{s}+0.94}{38.46\mathrm{s}^2+8.21\mathrm{s}+1} & \dfrac{-0.5}{25\mathrm{s}+1} \\ \dfrac{0.5}{25s+1} & \dfrac{0.044\mathrm{s}+0.88}{31.2\mathrm{s}^2+5.15\mathrm{s}+1} \end{bmatrix}
\end{aligned}
\tag{38}
$$

Model 2

$$
\begin{aligned}
G_1^2(s) &= \begin{bmatrix} \dfrac{0.0466\mathrm{s}+0.931}{109.2\mathrm{s}^2+11.83\mathrm{s}+1} & \dfrac{0.3}{25\mathrm{s}+1} \\ \dfrac{-0.3}{25s+1} & \dfrac{0.0560\mathrm{s}+1.131}{27.78\mathrm{s}^2+10.91\mathrm{s}+1} \end{bmatrix} \\
G_2^2(s) &= \begin{bmatrix} \dfrac{0.0466\mathrm{s}+0.922}{46.5\mathrm{s}^2+8.76\mathrm{s}+1} & \dfrac{0.4}{25\mathrm{s}+1} \\ \dfrac{-0.4}{25s+1} & \dfrac{0.0456\mathrm{s}+0.912}{61.06\mathrm{s}^2+11.41\mathrm{s}+1} \end{bmatrix} \\
G_3^2(s) &= \begin{bmatrix} \dfrac{0.0446\mathrm{s}+0.893}{38.46\mathrm{s}^2+8.21\mathrm{s}+1} & \dfrac{0.5}{25\mathrm{s}+1} \\ \dfrac{-0.5}{25s+1} & \dfrac{0.0418\mathrm{s}+0.836}{31.2\mathrm{s}^2+5.15\mathrm{s}+1} \end{bmatrix}
\end{aligned}
\tag{39}
$$

Controller design for switched system, case B

Controller design which uses equivalent subsystem method will be presented in details by controller design for mode 1. Nominal model was calculated from operating points of the mode 1 as the transfer function matrix with average parameters:

$$G^1(s) = \begin{bmatrix} \dfrac{0.0483s + 0.963}{64.72s^2 + 9.6s + 1} & \dfrac{-0.4}{25s + 1} \\ \dfrac{0.4}{25s + 1} & \dfrac{0.05s + 0.995}{40.01s^2 + 9.16s + 1} \end{bmatrix}. \tag{40}$$

Matrix $-G_m(s)$ contains off-diagonal elements of the matrix (40) and zero elements on diagonal. From the matrix $-G_m(s)$, frequency domain characteristic functions were obtained and plotted as in Fig. 5. Bode characteristics of equivalent models calculated

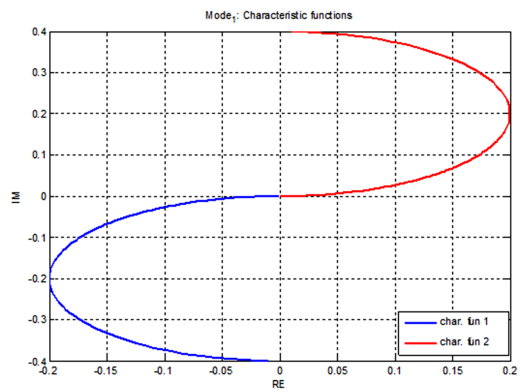

Figure 5. Characteristic functions, mode 1.

according to (11) and using both characteristic functions are depicted in Fig. 6 and 7. Phase margins of equivalent subsystems calculated using characteristic functions are compared in Tab. 1. According to the phase margins given in Tab. 1, equivalent subsys-

Table 3. Mode 1. Comparison of equivalent subsystem phase margin.

	Characteristic function 1	Characteristic function 2
Phase margin, subsystem 1	127.64	153.16
Phase margin, subsystem 2	138.05	151.06

tems calculated using characteristic function 2 are used to controller design. For each subsystem SISO controller design method which ensures desired phase margin is used.

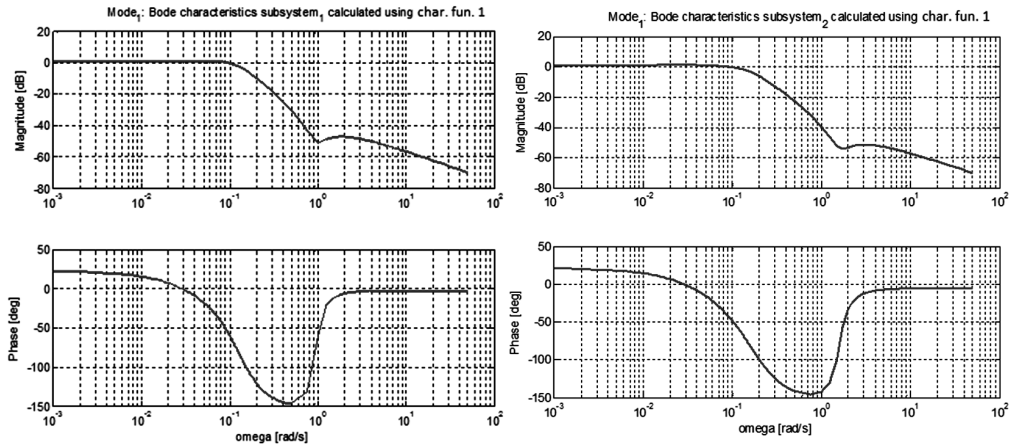

Figure 6. Equivalent models calculated using characteristic function 1.

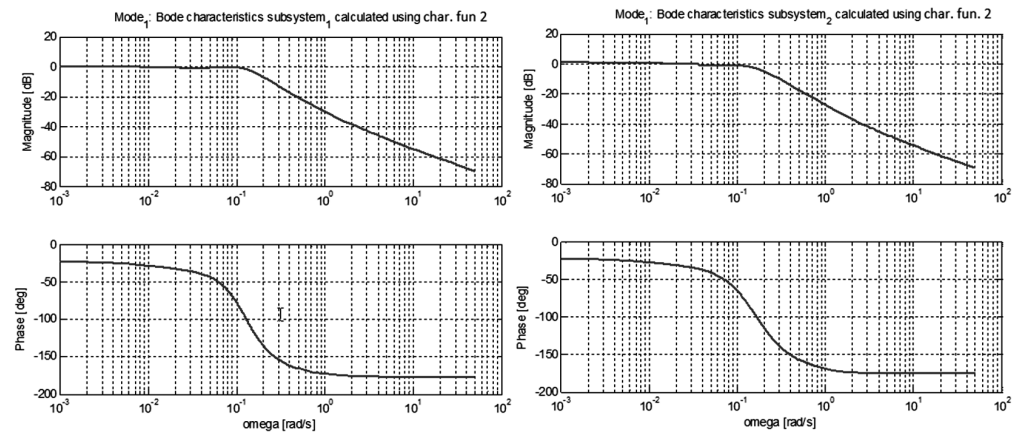

Figure 7. Equivalent models calculated using characteristic function 2.

The aim of SISO controller design is to ensure overshoot-free response, thus the nominal model phase margin is set on $PM = 70^0$. Respective Bode diagrams for subsystems with the controllers in open loop are presented in Fig. 8. There is indicated about 0 dB point on the magnitude diagrams. The frequency which corresponds to this point is also indicated in the phase diagrams, showing about -110^0. This proves phase margin $PM = 70^0$. Parameters of decentralized controller which ensures phase margin $PM = 70^0$ for both

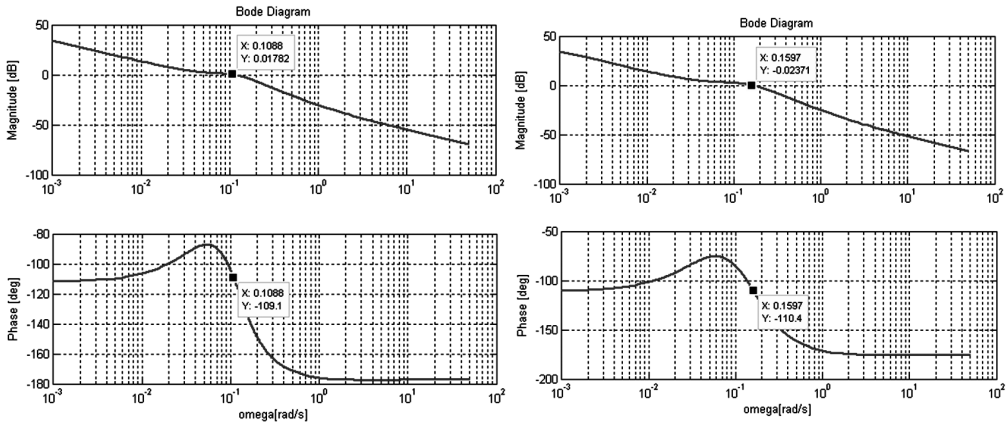

Figure 8. Bode characteristics for subsystem with controller, both subsystems have desired phase margin.

equivalent subsystems are as follows

$$R_1(s) = \begin{bmatrix} \dfrac{s+0.047}{s} & 0 \\ 0 & \dfrac{0.87s+0.078}{s} \end{bmatrix}. \tag{41}$$

To verify robust stability condition, additive uncertainty $l_a^1(\omega)$ is calculated according (34). Robust stability condition for both subsystems is depicted in Fig. 9. It is clear from Fig. 9 that robust stability condition is fulfilled. Nominal model simulation (Fig. 10)

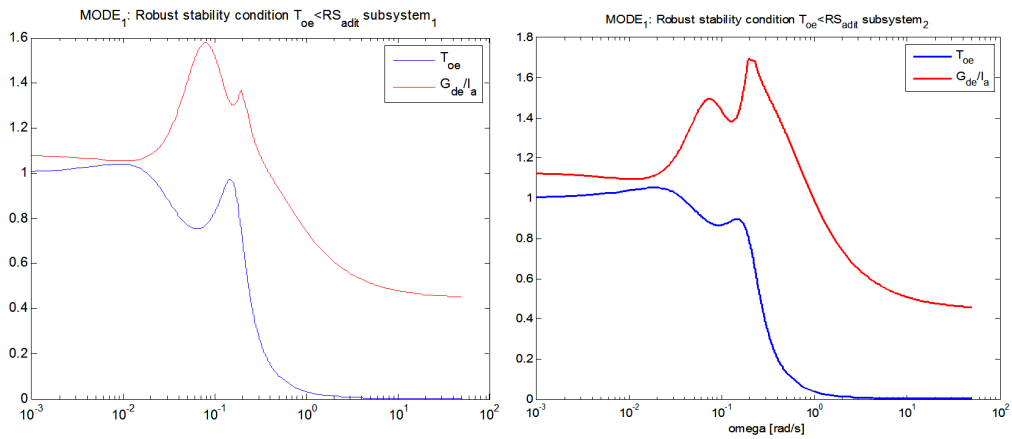

Figure 9. Bode characteristics for subsystem with controller, both subsystems have desired phase margin.

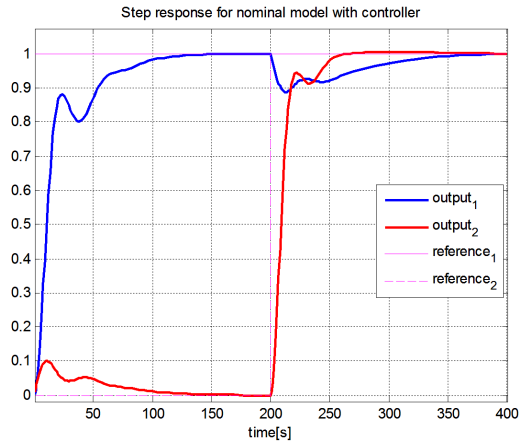

Figure 10. Nominal model simulation.

shows that decentralized controller for mode 1 ensures step response without overshoot. Based on the nominal model simulation, further controller deign will be considered in the context of overshoot-free response.

Mode 2

Nominal model for mode 2 was calculated from the transfer function matrices (39) as average one:

$$G^2(s) = \begin{bmatrix} \dfrac{0.0466s + 0.915}{64.72s^2 + 9.6s + 1} & \dfrac{-0.4}{25s + 1} \\ \dfrac{0.4}{25s + 1} & \dfrac{0.0478s + 0.96}{40.01s^2 + 9.16s + 1} \end{bmatrix}. \tag{42}$$

Controller for the mode 2 is designed in the same way as the controller for the mode 1. Phase margins of equivalent subsystems calculated using both characteristic functions are presented in Tab. 2 Characteristic function 2 is used for equivalent subsystems cal-

Table 4. Mode 2. Comparison of equivalent subsystem phase margin calculated using both characteristic functions.

	Characteristic function 1	Characteristic function 2
Phase margin, subsystem 1	138.72	155.71
Phase margin, subsystem 2	146.88	153.75

culation due to higher phase margin. Controllers for subsystems are again designed to

ensure phase margin $PM = 70^0$. Parameters of designed decentralized controller are as follows:

$$R_2(s) = \begin{bmatrix} \dfrac{1.29s+0.02}{s} & 0 \\ 0 & \dfrac{1.175s+0.071}{s} \end{bmatrix}. \tag{43}$$

to verify robust stability condition, additive uncertainty $l_a^2(\omega)$ was calculated according to (34). Robust stability condition for both subsystems is depicted in Fig. 11 and proves robust stability.

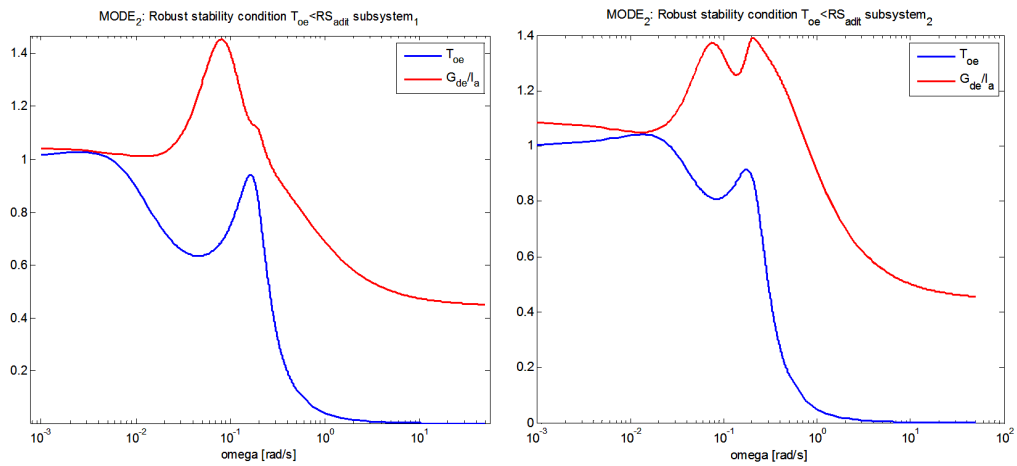

Figure 11. Robust stability condition for subsystem 1 and subsystem 2, mode 2.

Controller design for switched system, case A

In this case, nominal model is calculated from all operating points of both modes (38) and (39). Interactions in mode 1 have opposite sign to the interactions in mode 2, thus by nominal model calculation, interactions cancels and phase margin of equivalent subsystems is equal in both characteristic functions (Tab. 3).

Nominal model for all operating points obtained from both modes is as follows

$$G(s) = \begin{bmatrix} \dfrac{0.047\mathrm{s}+0.939}{64.72\mathrm{s}^2+9.6\mathrm{s}+1} & 0 \\ 0 & \dfrac{0.0491\mathrm{s}+0.985}{40.01\mathrm{s}^2+9.16\mathrm{s}+1} \end{bmatrix}. \tag{44}$$

To design robust control desired phase margin was chosen $PM = 70^0$. Parameters of

Table 5. Equivalent subsystem phase margin comparison.

	Characteristic function 1	Characteristic function 2
Phase margin, subsystem 1	138.1	138.1
Phase margin, subsystem 2	179.48	179.48

designed decentralized controller are given below

$$R(s) = \begin{bmatrix} \dfrac{0.75s+0.07}{s} & 0 \\ 0 & \dfrac{0.99s+0.095}{s} \end{bmatrix}. \tag{45}$$

By robust stability condition verification, additive uncertainty $l_a(\omega)$ was calculated according to (19). Robust stability condition for both subsystems is depicted in Fig. 12. Robust stability condition is fulfilled. Both approaches to controller design were com-

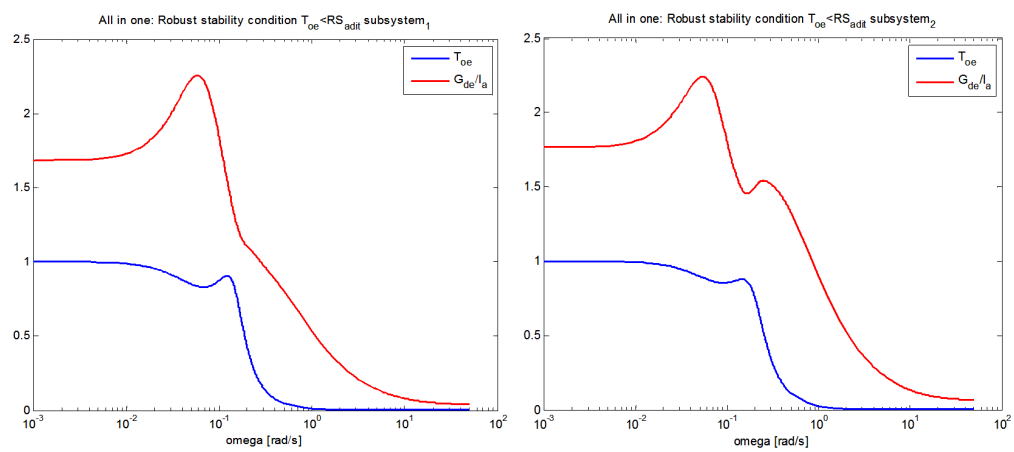

Figure 12. Robust stability condition for subsystem 1 and subsystem 2.

pared by simulation with several step changes of reference value. Results are presented in Fig. 13 (zoomed in Fig. 14). Plots of the corresponding control signals are presented in Fig. 15. Simulation in different operating points (fig. 13 and 14) shows that the system with robust hybrid control (case B) responses without overshoot and has the same settling time as system with robust control (case A). On the other hand, significant overshoot characterizes responses of tank 1 being controlled by the robust controller (case A).

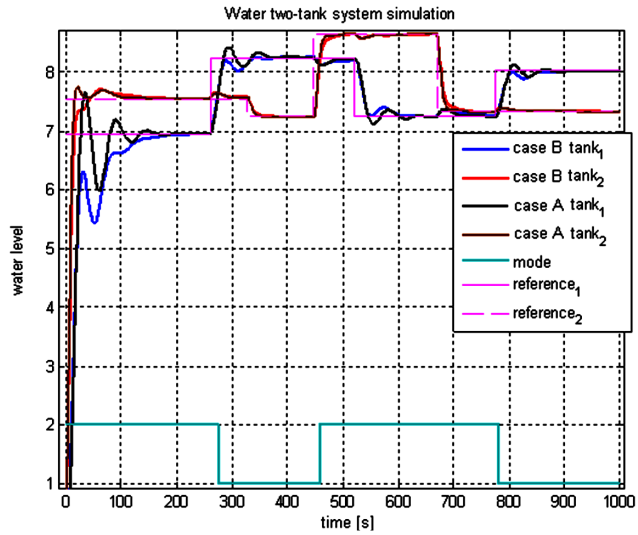

Figure 13. Comparison of robust hybrid and pure robust control.

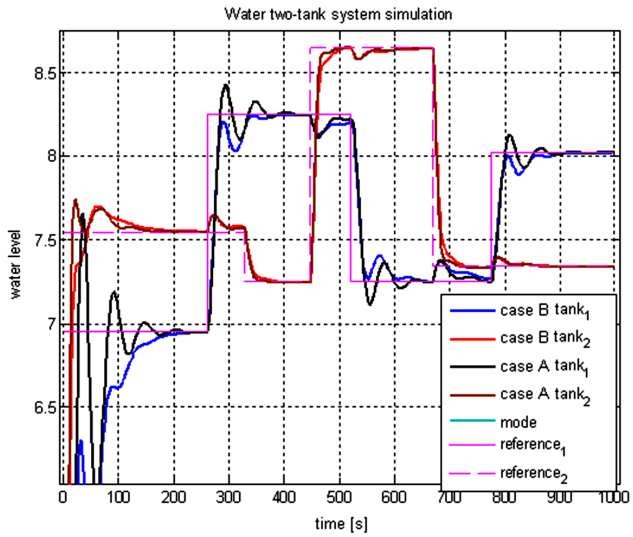

Figure 14. Comparison of robust hybrid and pure robust control, detail of Fig. 13.

5. Conclusion

In this paper two robust control approaches and unification of robust control design for SISO and MIMO systems were presented. Comparison of robust control (case A) and

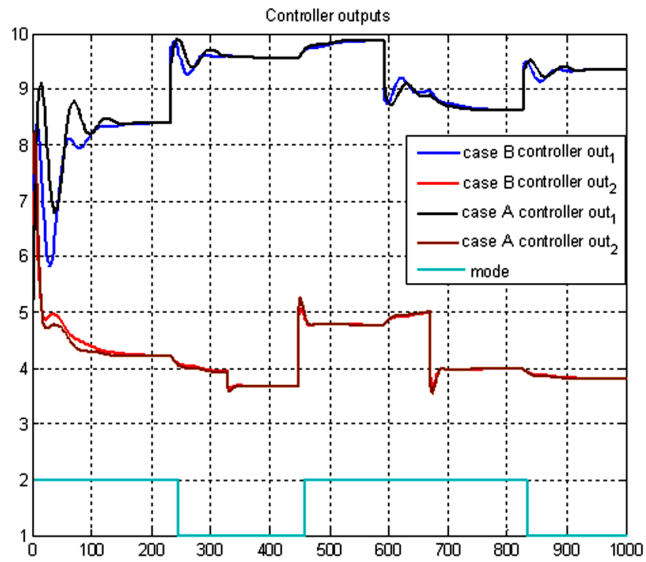

Figure 15. Controllers outputs comparison.

robust hybrid control (case B) shows better performance of the latter on (Fig. 13, 14). Comparison of robust stability conditions for both cases shows that uncertainties for robust hybrid control (case B) are higher so this approach is more conservative. Robust hybrid control (case B) brings better performance if uncertainties are small enough to fulfill robust stability condition (23) or (28) by the controller design.

References

[1] M.S. BRANICKY, V.S. BORKAR and S.K. MITTER: A unified framework for hybrid control: model and optimal control theory. *IEEE Trans. on Automatic Control*, **43**(1), (1998) 31-45.

[2] C. CAI , R. GOEBEL and A.R. TEEL: Smooth Lyapunov functions for hybrid systems, Part I: Existence is equivalent to robustness. *IEEE Trans. on Automatic Control*, **52**(7), (2007), 1264-1277.

[3] R. GOEBEL and A.R. TEEL: Solutions to hybrid inclusions via set and graphical konvergence with stability theory applications. *Automatica*, **42**(4), (2006) 573-587.

[4] A. KOZÁKOVÁ, V. VESELÝ, J. OSUSKÝ: A New Nyquist-based technique for tuning robust decentralized controllers. *Kybernetika*, **45**(1), (2009), 63-83, ISSN 0023-5954.

[5] D. LIBERZON: Switching in systems and control. Birkhauser, 2003.

[6] J. LUNZE and F.L. LAGARRIGUE: Hanbook of hybrid systems control. Theory, tools, applications. Cambridge University Press, 2009.

[7] J. LYGEROS: On overview of research areas in hybrid systems control. *Proc. of the 44IEEE Conf. on Decission and Control and the European Control Conf.*, Spain, (2005), CDROM.

[8] J. MALMBORG: Analysis and design of hybrid control systems. Department of Automatic Control Lund Institute of Technology, Sweden, 1998, ISSN 0280-5316.

[9] S. SKOGESTAD and I. POSTLETHWAITE: Multivariable feedback control: analysis and design. (3rd edn.), John Wiley & Sons., 1997.